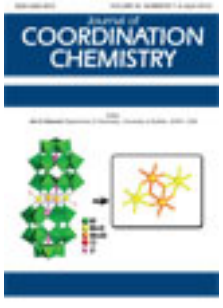

Journal of Coordination Chemistry
Publication details, including instructions for authors and subscription information:
http://www.tandfonline.com/loi/gcoo20

Design, synthesis, and characterization of a series of biologically active copper(II) Schiff-base coordination compounds

Ram N. Patel [a], Anurag Singh [a], Krishna K. Shukla [a], Vishnu P. Sondhiya [a], Dinesh K. Patel [a], Yogendra Singh [a] & Rajesh Pandey [a]
[a] Department of Chemistry, A.P.S. University, Rewa, Madhya Pradesh 486003, India
Published online: 30 Mar 2012.

To cite this article: Ram N. Patel, Anurag Singh, Krishna K. Shukla, Vishnu P. Sondhiya, Dinesh K. Patel, Yogendra Singh & Rajesh Pandey (2012) Design, synthesis, and characterization of a series of biologically active copper(II) Schiff-base coordination compounds, Journal of Coordination Chemistry, 65:8, 1381-1397, DOI: 10.1080/00958972.2012.673221

To link to this article: http://dx.doi.org/10.1080/00958972.2012.673221

Journal of Coordination Chemistry
Vol. 65, No. 8, 20 April 2012, 1381–1397

Design, synthesis, and characterization of a series of biologically active copper(II) Schiff-base coordination compounds

RAM N. PATEL*, ANURAG SINGH, KRISHNA K. SHUKLA, VISHNU P. SONDHIYA, DINESH K. PATEL, YOGENDRA SINGH and RAJESH PANDEY

Department of Chemistry, A.P.S. University, Rewa, Madhya Pradesh 486003, India

(*Received 22 November 2011; in final form 25 January 2012*)

Four Schiff-base copper(II) complexes, $[Cu(L^1)(Phen)(H_2O)](NO_3)_2$ (**1**), $[Cu(L^1)(bipy)(H_2O)](ClO_4)(H_2O)(NO_3)$ (**2**), $[Cu(L^1)(Dien)](ClO_4)_2(H_2O)$ (**3**), and $[Cu(L^1)(ImH)(H_2O)](ClO_4)$ (**4**) ($\mathbf{L^1}$ = N-[(1)-pyridin-2-ylmethylidene]benzohydrazide, Phen = 1,10-phenanthroline, bipy = 2, 2′-bipyridine, Dien = diethylenetriamine, ImH = imidazole), have been synthesized and characterized using various physico-chemical techniques. $\mathbf{L^1}$ is coordinated to copper(II) neutral and uninegatively charged tridentate chelating agent *via* the azomethine nitrogen, pyridine nitrogen, and carbonyl oxygen. The copper(II) complexes are paramagnetic with octahedral stereochemistry. The crystal structures of the complexes reveal the presence of structure consisting of a tridentate N, N, O donor Schiff base, tridentate NNN donor polyamine or N, N donor heterocyclic base and the copper(II) center. In **1**, **2**, and **4,** water is present as a coordinating molecule whereas in **2** and **4** it is also present as lattice water. In discrete monomeric species all complexes show significant hydrogen-bonding interactions. H-bridges are also present in the solid state structure. Complexes **1**–**4** effectively catalyze the dismutation of superoxide (O_2^-) in alkaline nitro blue tetrazolium assay and IC_{50} values were determined. The susceptibility of certain strains of bacteria toward the precursors $\mathbf{L^1}$ and their complexes were also evaluated.

Keywords: Copper(II) complexes; Crystal structure; H-bonding; EPR spectra

1. Introduction

Schiff bases are widely studied because of increasing recognition of their role in biological systems [1]. Their complexes are used in some chemical processes as catalysts and as biological models, emulating activity of proteins [2]. Copper(II) complexes as anti-inflammatory drugs are often more active than the parent ligands [3] and work has appeared concerning models of copper enzymes [4]. Mixed ligand complexes formed between metal ions, Schiff bases and hetero aromatic nitrogen bases may be considered as models for substrate metal ion–enzyme interaction. Chelation causes changes in the biological properties of the ligands and also the metal. A number of Schiff-base complexes [5] have been tested for antibacterial activities, antibacterial [6], antifungal [6, 7], anticancer [8], and herbicidal [9] activities.

*Corresponding author. Email: rnp64@ymail.com

ISSN 0095-8972 print/ISSN 1029-0389 online
http://dx.doi.org/10.1080/00958972.2012.673221

As extension of our previous work [10, 11], we designed a tridentate NNO donor Schiff base ligand and its ternary copper(II) complexes, namely $[Cu(L^1)(Phen)(H_2O)](NO_3)_2$ (**1**), $[Cu(L^1)(bipy)(H_2O)](ClO_4)(H_2O)(NO_3)$ (**2**), $[Cu(L^1)(Dien)](ClO_4)_2(H_2O)$ (**3**), and $[Cu(L^1)(ImH)(H_2O)](ClO_4)$ (**4**). Structures of all complexes have been solved by single-crystal X-ray crystallography and the biological activities of the complexes have also been investigated.

2. Experimental

2.1. *Materials*

Copper(II) nitrate trihydrate was purchased from S.D. fine-chemicals, India. All other chemicals were of synthetic grade and used without purification.

2.2. *Physical measurement*

2.2.1. Elemental analysis. Elemental analyses of the complexes were performed on an Elementar Vario EL III Carlo Erba 1108 analyzer. FAB mass spectra were recorded on a JEOL SX 102/DA 6000 mass spectrometer/data system using xenon (6 kV, 10 mA) as the FAB gas. The accelerating voltage was 10 kV and the spectra were recorded at room temperature.

2.2.2. Spectroscopy. UV-Vis spectra were recorded at 25°C on a Shimadzu UV-Visible recording spectrophotometer UV-1601 in quartz cells. Infrared (IR) spectra were recorded in KBr on a Perkin-Elmer 783 spectrophotometer. X-band electron paramagnetic resonance (EPR) spectra were recorded with a Varian E-line Century Series Spectrometer equipped with a dual cavity and operating at X-band (~9.4 GHz) with 100 kHz modulation frequency. TCNE was used as field marker. The Varian quartz tubes were used for measuring EPR spectra of polycrystalline samples and frozen solutions.

2.2.3. Magnetic susceptibility. Magnetic susceptibility measurements were made on a Gouy balance using a mercury(II) tetrathiocyanato cobaltate(II) as calibrating agent ($\chi_g = 16.44 \times 10^{-6}$ c.g.s. units).

2.2.4. Electrochemistry. Cyclic voltammetry was carried out with a BAS-100 Epsilon electrochemical analyzer having an electrochemical cell with a three-electrode system. Ag/AgCl was used as a reference electrode, glassy carbon as working electrode, and platinum wire as an auxiliary electrode; 0.1 mol L^{-1} $NaClO_4$ was used as supporting electrolyte and DMSO as solvent. All measurements were carried out at 298 K under a nitrogen atmosphere.

2.2.5. Superoxide dismutase activity. The *in-vitro* superoxide dismutase (SOD) activity was measured using alkaline DMSO as a source of superoxide radical (O_2^-) and nitro blue tetrazolium (NBT) chloride as O_2^- scavenger [12]. In general, 400 µL sample to be assayed was added to a solution containing 2.1 mL of 0.2 mol L^{-1} potassium phosphate buffer (pH 8.6) and 1 mL of 56 µmol L^{-1} alkaline DMSO solution was added while stirring. The absorbance was then monitored at 540 nm against a sample prepared under similar condition except NaOH was absent in DMSO. A unit of SOD activity is the concentration of complex, which causes 50% inhibition of alkaline DMSO mediated reduction of NBT.

2.2.6. Antibacterial activity measurements. The *in-vitro* antibacterial activities of these complexes were tested using the paper disc diffusion method [13]. Autoclaved (20 min at 121°C and at 15 lb pressure) nutrient agar medium was poured into sterile Petri disc and allowed to solidify. Petri dishes were seeded with bacterial species and paper discs were placed at the dish after dipping into test compound (DMSO solution). The width of the growth inhibition zone around the disc was measured after 24 h incubation at 37°C.

2.3. *Synthesis*

2.3.1. Synthesis of L^1. The Schiff base was synthesized by reacting benzoylhydrazide (136.1 mg, 10.0 mmol) and 2-pyridenecarboxaldehyde (107.1 mg, 10.0 mmol) in ethanol [14]. The resulting solution was refluxed for 4 h. The product was recrystallized in high yield from hot ethanol. Yield: 226.1 mg (93%). Anal. Calcd for $C_{13}H_{11}N_3O$ (%): C, 69.25; H, 4.88; N, 18.64. Found (%): C, 69.02; H, 4.56; N, 18.45.

2.3.2. Synthesis of $[Cu(L^1)(Phen)(H_2O)](NO_3)_2$ (1). L^1 (225 mg, 1.0 mmol) was dissolved in 10 mL methanol. After stirring 10 min, $CuNO_3 \cdot 3H_2O$ (242 mg, 1.0 mmol) was added dropwise and the color of solution changed to green. After 1 h stirring phen (198 mg, 1.0 mmol) was also added dropwise. The reaction mixture was further stirred for 3 h. After 3 h stirring, the reaction mixture was filtered and allowed to stand at room temperature for a few days. Dark green needle-shaped crystals appear by slow evaporation of a solution of **1**. Yield: 565 mg (85%). Anal. Calcd for $C_{25}H_{21}CuN_7O_8$ (%): C, 49.09; H, 3.43; N, 16.03. Found (%): C, 48.89; H, 3.11; N, 15.86.

2.3.3. $[Cu(L^1)(bipy)(H_2O)](ClO_4)(H_2O)(NO_3)$ (2). Complex **2** was synthesized following the same procedure as for **1**, only bipy (156 mg, 1.0 mmol) was added in place of phen. After stirring for 30 min, $NaClO_4$ (122 mg, 1.0 mmol) was added dropwise and the reaction mixture was further stirred for 3 h. After 3 h stirring, reaction mixture was filtered and dried at room temperature. Dark green needle-shaped crystals appear by slow evaporation of a solution of **2** in methanol after 3 days at room temperature. Yield: 581 mg (78%). Anal. Calcd for $C_{23}H_{19}ClCuN_6O_{10}$ (%): C, 43.23; H, 2.97; N, 13.15. Found (%): C, 43.01; H, 2.67; N, 13.01.

2.3.4. [Cu(L^1)(Dien)](ClO_4)$_2$(H_2O) (3). L^1 (225 mg, 1.0 mmol) was dissolved in 10 mL methanol. After stirring 10 min, $CuNO_3 \cdot 3H_2O$ (242 mg, 1.0 mmol) was added dropwise and the color of solution changed to green. After 1 h stirring dien (103 mg, 1.0 mmol) was also added dropwise and stirred for 30 min. Then $NaClO_4$ (244 mg, 2.0 mmol) was added dropwise and the reaction mixture was further stirred for 3 h. The solution was filtered and allowed to stand at room temperature for a few days. Blue crystals formed which were filtered off and dried in air. Yield: 626 mg (77%). Anal. Calcd for $C_{17}H_{26}Cl_2CuN_6O_{10}$ (%): C, 33.50; H, 4.27; N, 13.79. Found (%): C, 33.35; H, 4.01; N, 13.59.

2.3.5. [Cu(L^1)(ImH)(H_2O)](ClO_4) (4). Complex **4** was synthesized following the same procedure as **2**, only ImH (68 mg, 1.0 mmol) was added in place of bipy. Slow evaporation of the reaction mixture yielded good quality blue crystals in a few days. Yield: 585 mg (89%). Anal. Calcd for $C_{16}H_{15}ClCuN_5O_6$ (%): C, 40.65; H, 3.17; N, 14.83. Found (%): C, 40.31; H, 2.95; N, 14.68.

2.3.6. Crystal structure determination. Crystals suitable for single crystal X-ray analysis for all the complexes were grown by slow evaporation of the reaction mixture at room temperature. Single crystals suitable for single-crystal X-ray diffraction of **1**, **2**, and **3** were mounted on glass fibers and used for data collection. Crystal data were collected on an Enraf-Nonius $MACH_3$ diffractometer using graphite monochromated Mo-Kα radiation ($\lambda = 0.71073$ Å). The crystal orientation, cell refinement, and intensity measurements were made using CAD-4PC performing ψ-scan measurements. The structures were solved by direct methods using SHELXS-97 [15] and refined by full-matrix least-squares against F^2 using SHELXL-97 [16]. All non-hydrogen atoms were refined anisotropically. All hydrogen atoms were geometrically fixed and allowed to refine using a riding model.

3. Results and discussion

3.1. *Synthesis*

All the complexes and L^1 were synthesized by the following routes (scheme 1). These complexes were obtained in good yield and characterized by microanalysis and FAB^+ mass spectrometry. The complexes are stable in the solid state and soluble in common organic solvents.

3.2. *Single-crystal X-ray diffraction*

The copper(II) complexes were structurally characterized using single-crystal X-ray diffraction. Crystallographic data and structure refinement parameters are summarized in table 1. Selected bond lengths and angles are listed in table 2. Complex **1** crystallizes as green crystals in the monoclinic crystal system having space group *Cc* with four molecules in the unit cell. The ORTEP view of **1** is given in figure 1. X-ray analysis shows that copper(II) in **1** is coordinated by four nitrogen atoms and one oxygen atom.

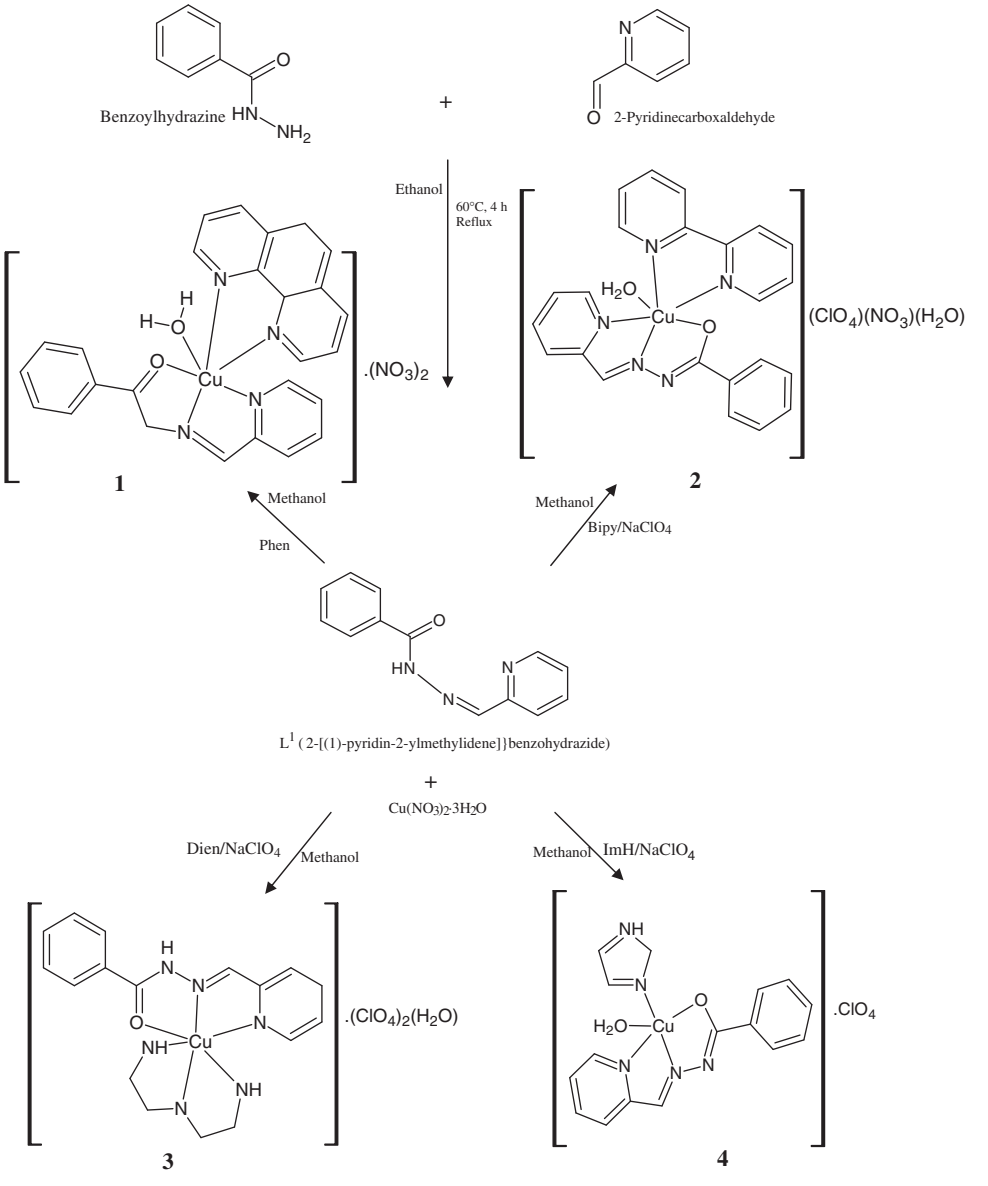

Scheme 1. Synthesis of **1**, **2**, **3**, and **4**.

Two neutral tridentate ligands are coordinated meridonial [17]. The Cu–$N_{pyridine}$ bond distances in **1** (average, Cu–N = 2.0976 Å) are similar to Cu–N pyridine distances determined for other mononuclear copper(II) complexes [18]. Based on the corresponding bond lengths and angles, the local coordination geometry around copper(II) can be described as a distorted octahedron. The structure of **2** is illustrated in figure 2. The asymmetric unit of **2** consists of $[Cu(L^1)(bipy)(H_2O)]^{2+}$, one ClO_4^-, one NO_3^-, and water molecules. Complex **3** is light blue crystals that belong to the monoclinic space group $P2_1/n$ with four molecules in the unit cell. The ORTEP view [19] of the complex is

Table 1. Crystal structure refinement parameters of **1–4**.

	1	**2**	**3**	**4**
Empirical formula	C_{25} $H_{21}CuN_7$ O_8	$C_{23}H_{19}ClCuN_6O_{10}$	$C_{17}H_{26}Cl_2CuN_6O_{10}$	$C_{16}H_{15}ClCuN_5O_6$
Formula weight	611.03	638.43	608.88	472.32
Temperature (K)	150(2)	120(2)	120(2)	120(2)
Wavelength (Å)	0.71073	0.71073	0.71073	0.71073
Crystal system	Monoclinic	Orthorhombic	Monoclinic	Triclinic
Space group	*Cc*	*Pna*21	$P2_1/n$	*P*-1
Unit cell dimensions (Å, °)				
a	11.9844(12)	12.3600(6)	14.0169(11)	8.085(2)
b	17.2683(17)	17.5933(11)	11.3256(10)	10.117(2)
c	12.2529(13)	12.3203(6)	15.8019(11)	13.251(4)
α	90	90	90	105.21(2)
β	91.574(9)	90	106.143(8)	107.74(3)
γ	90	90	90	99.53(2)
Volume (Å^3), *Z*	2534.8(4), 4	2679.1(2), 4	2409.6(3), 4	960.0(4), 2
Calculated density (g cm^{-3})	1.601	1.583	1.678	1.634
F(000)	1252	1300	1252	480
Crystal size (mm^3)	0.23 × 0.18 × 0.15	0.32 × 0.28 × 0.24	0.23 × 0.18 × 0.15	0.28 × 0.23 × 0.15
θ range for data collection (°)	3.33–25.00	3.29–25.00	3.03–25.00	3.01–25.00
Index range	$-14 \le h \le 10$; $-20 \le k \le 20$; $-14 \le l \le 14$	$-14 \le h \le 14$; $-20 \le k \le 20$; $-14 \le l \le 14$	$-16 \le h \le 15$; $-13 \le k \le 13$; $-18 \le l \le 18$	$-7 \le h \le 9$; $-12 \le k \le 12$; $-15 \le l \le 15$
Refinement method	Full-matrix least-squares on F^2	Full-matrix least-squares on F^2	Full-matrix least-squares on F^2	Full-matrix least-squares on F^2
Data/restraints/parameters	3414/2/378	4691/1/370	4249/0/353	3365/0/262
Goodness-of-fit on F^2	1.015	1.030	0.941	1.123
Final *R* indices [$I > \sigma(I)$]	$R_1 = 0.0297$, $wR_2 = 0.0715$	$R_1 = 0.0469$, $wR_2 = 0.1250$	$R_1 = 0.0290$, $wR_2 = 0.0711$	$R_1 = 0.1274$, $wR_2 = 0.4037$
R indices (all data)	$R_1 = 0.0321$, $wR_2 = 0.0724$	$R_1 = 0.0536$, $wR_2 = 0.1274$	$R_1 = 0.0432$, $wR_2 = 0.0734$	$R_1 = 0.1636$, $wR_2 = 0.4141$

shown in figure 3. X-ray analysis shows that the copper(II) in **3** has distorted octahedral geometry. From the structure it is also clear that the three donors of $\mathbf{L^1}$ lie in the plane. The structure of **4** is shown in figure 4. The complex crystallizes in the triclinic space group *P*-1 with two molecules in the unit cell. Copper(II) is coordinated by two nitrogen atoms and one deprotonated carbonyl oxygen atom of $\mathbf{L^1}$, one nitrogen atom from imidazole, and one oxygen atom from water. The trigonal index τ is calculated for **4** using the equation $\tau = (\beta - \alpha)/60$ [20–22] (for perfect square-pyramidal and trigonal-bipyramidal geometries the value of τ are zero and unity, respectively). The value of τ is 0.23, indicating distorted square-pyramidal geometry.

Conventional hydrogen-bonding is present in all the copper(II) complexes (table 3). O–H···O and N–H···O intermolecular and intramolecular hydrogen-bonding stabilizes the structures of the complexes. Nitrate forms relatively weaker hydrogen bonds with coordinated water in **1**.

3.3. *Electronic spectra*

The reflectance spectra of the four complexes show resolved d–d bands at 620, 700, 680, and 675 nm, respectively, for **1–4**. Electronic spectra for the complexes recorded in

Table 2. Selected bond lengths (Å) and angles (°) for **1–4**.

1			
Cu(1)–O(101)	1.959(2)	Cu(1)–N(2)	2.062(3)
Cu(1)–N(4)	2.015(3)	Cu(1)–N(1)	2.292(3)
Cu(1)–N(5)	2.021(3)	Cu(1)–O(1)	2.460(5)
N(2)–Cu(1)–O(1)	70.85(3)	N(1)–Cu(1)–O(1)	145.52(6)
N(5)–Cu(1)–O(1)	98.69(2)	N(4)–Cu(1)–O(1)	82.64(3)
O(101)–Cu(1)–O(1)	89.94(1)	O(101)–Cu(1)–N(5)	94.93(12)
O(101)–Cu(1)–N(4)	171.41(13)	O(101)–Cu(1)–N(2)	87.98(11)
N(4)–Cu(1)–N(5)	82.02(12)	N(5)–Cu(1)–N(2)	169.17(12)
N(4)–Cu(1)–N(2)	93.60(11)	N(4)–Cu(1)–N(1)	94.29(11)
O(101)–Cu(1)–N(1)	94.27(11)	N(2)–Cu(1)–N(1)	75.11(11)
N(5)–Cu(1)–N(1)	114.97(11)	C(1)–N(1)–Cu(1)	132.0(2)
C(5)–N(1)–Cu(1)	110.3(2)	N(3)–N(2)–Cu(1)	120.1(2)
C(6)–N(2)–Cu(1)	120.1(2)	C(25)–N(4)–Cu(1)	112.2(2)
C(14)–N(4)–Cu(1)	129.0(3)	C(23)–N(5)–Cu(1)	130.1(3)
C(24)–N(5)–Cu(1)	111.9(2)		
2			
Cu(1)–N(2)	1.969(3)	Cu(1)–O(2)	2.001(4)
Cu(1)–N(4)	2.044(4)	Cu(1)–N(3)	2.283(4)
Cu(1)–N(1)	2.008(4)	Cu(1)–O(1)	2.383(3)
N(2)–Cu(1)–O(2)	94.48(16)	N(2)–Cu(1)–O(1)	107.87(18)
N(2)–Cu(1)–N(1)	81.48(18)	O(2)–Cu(1)–O(1)	87.32(14)
O(2)–Cu(1)–N(1)	173.09(16)	N(1)–Cu(1)–O(1)	88.59(15)
N(2)–Cu(1)–N(4)	178.29(18)	N(4)–Cu(1)–O(1)	72.45(16)
O(2)–Cu(1)–N(4)	87.21(15)	N(3)–Cu(1)–O(1)	147.30(13)
N(1)–Cu(1)–N(4)	96.87(16)	C(17)–O(1)–Cu(1)	110.2(3)
N(2)–Cu(1)–N(3)	104.54(18)	C(1)–N(1)–C(5)	119.9(5)
O(2)–Cu(1)–N(3)	94.43(15)	C(1)–N(1)–Cu(1)	126.0(3)
N(1)–Cu(1)–N(3)	92.02(16)	C(5)–N(1)–Cu(1)	114.0(3)
N(4)–Cu(1)–N(3)	75.02(16)		
3			
Cu(1)–N(5)	1.998(2)	Cu(1)–N(2)	2.055(2)
Cu(1)–N(6)	2.020(2)	Cu(1)–N(1)	2.300(2)
Cu(1)–N(4)	2.020(2)	Cu(1)–O(1)	2.440(2)
N(5)–Cu(1)–N(6)	84.27(9)	C(1)–N(1)–Cu(1)	132.33(17)
N(5)–Cu(1)–N(4)	84.49(9)	C(5)–N(1)–Cu(1)	109.89(16)
N(6)–Cu(1)–N(4)	163.05(11)	C(6)–N(2)–Cu(1)	119.98(17)
N(5)–Cu(1)–N(2)	178.53(9)	N(3)–N(2)–Cu(1)	120.02(15)
N(6)–Cu(1)–N(2)	95.68(9)	C(17)–N(4)–Cu(1)	108.77(16)
N(4)–Cu(1)–N(2)	95.23(9)	C(14)–N(6)–Cu(1)	108.98(17)
N(5)–Cu(1)–N(1)	106.07(9)	C(15)–N(5)–Cu(1)	108.51(16)
N(6)–Cu(1)–N(1)	94.68(10)	N(1)–Cu(1)–O(1)	146.04(2)
N(4)–Cu(1)–N(1)	100.59(10)	N(2)–Cu(1)–O(1)	70.97(9)
N(2)–Cu(1)–N(1)	75.40(8)	C(16)–N(5)–Cu(1)	108.18(16)
N(6)–Cu(1)–O(1)	84.18(1)	N(4)–Cu(1)–O(1)	87.17(4)
N(5)–Cu(1)–O(1)	107.58(1)		
4			
Cu(1)–N(4)	1.945(13)	Cu(1)–N(1)	2.046(13)
Cu(1)–N(2)	1.945(14)	Cu(1)–O(101)	2.342(10)
Cu(1)–O(1)	1.990(11)		
N(4)–Cu(1)–N(2)	172.6(6)	N(1)–Cu(1)–O(101)	90.9(5)
N(4)–Cu(1)–O(1)	96.3(5)	C(7)–O(1)–Cu(1)	110.2(11)
N(2)–Cu(1)–O(1)	79.3(5)	N(1)–Cu(1)–O(101)	90.9(5)
N(4)–Cu(1)–N(1)	103.3(6)	C(7)–O(1)–Cu(1)	110.2(11)
N(2)–Cu(1)–N(1)	80.3(6)	C(6)–N(2)–Cu(1)	118.3(12)
O(1)–Cu(1)–N(1)	158.7(5)	N(3)–N(2)–Cu(1)	115.5(9)
N(4)–Cu(1)–O(101)	91.7(5)	C(14)–N(4)–Cu(1)	130.0(12)
N(2)–Cu(1)–O(101)	94.7(5)	C(16)–N(4)–Cu(1)	123.8(12)
O(1)–Cu(1)–O(101)	96.8(5)		

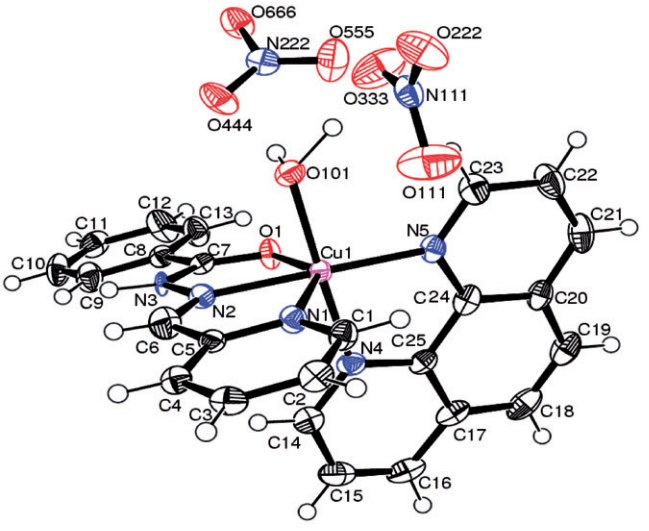

Figure 1. ORTEP view of $[Cu(L^1)(Phen)(H_2O)](NO_3)_2$ (**1**).

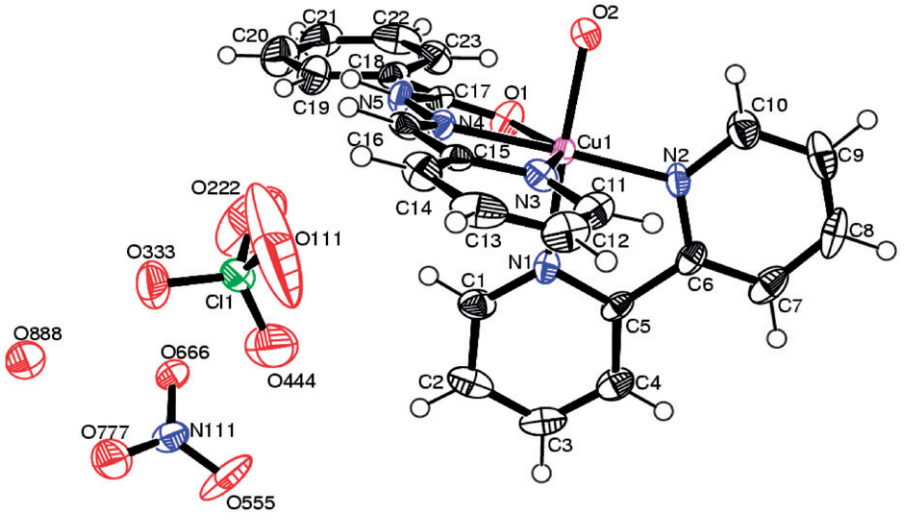

Figure 2. ORTEP view of $[Cu(L^1)(bipy)(H_2O)](ClO_4)(H_2O)(NO_3)$ (**2**).

DMSO (3×10^{-3} mol L^{-1}) are in good agreement with their geometries. The first absorption band ($d_{xy} \rightarrow d_{x^2-y^2}$) d–d band in the four complexes is in the range 620–680 nm and assigned to $^2B_{1g} \rightarrow {}^2B_{2g}$; the band at 380 ± 5 nm is attributed to $^2B_{1g} \rightarrow {}^2E_g$ transition, assigned to ligand-to-metal charge-transfer absorption [23]. UV-Vis spectra of saturated aqueous solutions of three complexes show the same maximum at 634 nm, indicating that in solution **1**, **2**, and **4** have the same chromophore as a result of coordination of water [24].

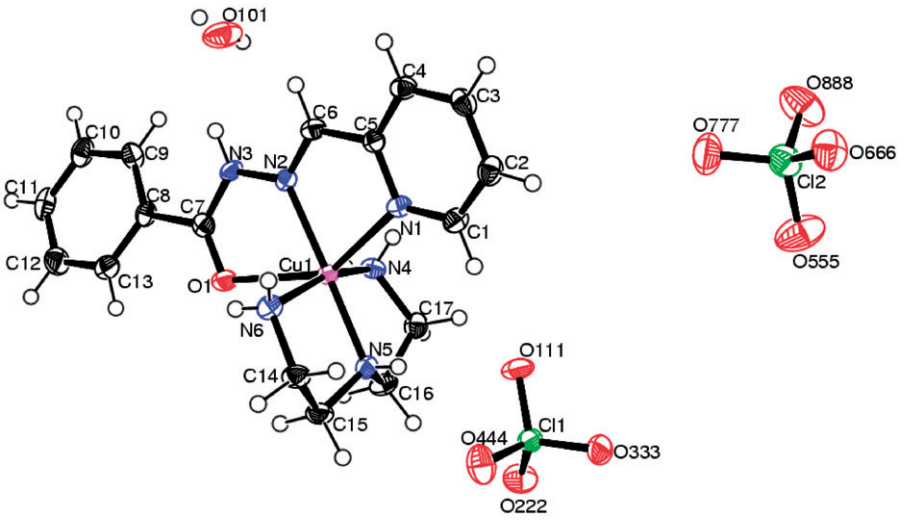

Figure 3. ORTEP view of $[Cu(L^1)(Dien)](ClO_4)_2(H_2O)$ (**3**).

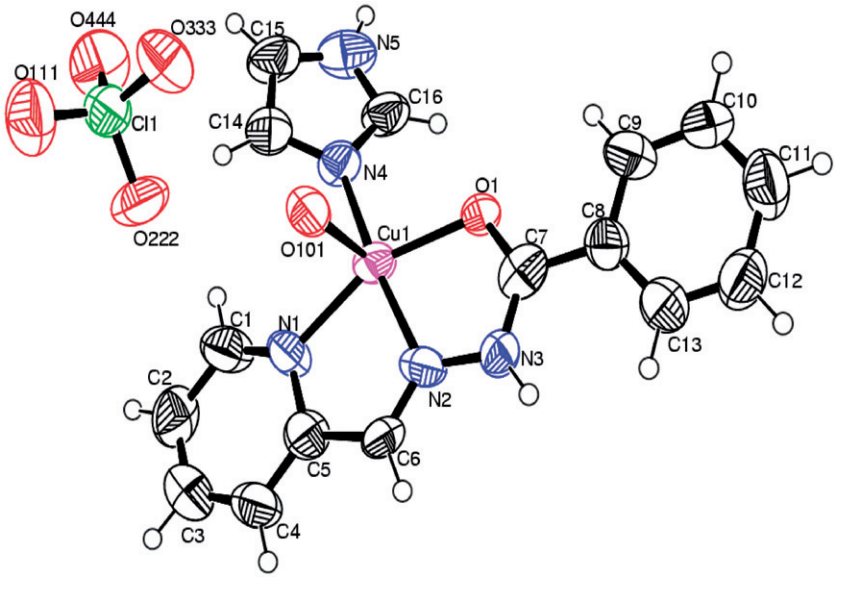

Figure 4. ORTEP view of $[Cu(L^1)(ImH)(H_2O)](ClO_4)$ (**4**).

3.4. *Magnetic moment*

The magnetic moment of 1.83 ± 0.05 B.M. is close to the values for copper(II) complexes without interactions [25]. The observed magnetic moments of these complexes, **1**, **2**, **3**, and **4** are 1.78, 1.79, 1.86, and 1.88, respectively, and are quite close to values for other copper(II) complexes [26]. These magnetic moment values are suggestive of distorted octahedral complexes [27].

Table 3. Hydrogen-bonding interactions (Å and °) for **1–4**.

D–H···A	D–H (Å)	H···A (Å)	D···A (Å)	∠D–H···A (°)	Symmetry
Intramolecular					
1					
O101–H102···O1 (0)	0.697(0.054)	2.938(0.058)	3.152(0.004)	101.51(5.14)	x, y, z
3					
N4–H4NA···N2 (0)	0.760(0.027)	2.985(0.025)	3.011(0.003)	84.66(2.00)	x, y, z
N6–H6NA···O1 (0)	0.735(0.030)	2.576(0.026)	3.006(0.003)	119.42(2.37)	x, y, z
Intermolecular					
1					
O101–H101···O333 (0)	1.182(0.079)	1.595(0.081)	2.749(0.006)	163.35(6.57)	x, y, z
O101–H102···O444 (0)	0.697(0.054)	2.021(0.054)	2.710(0.004)	169.70(5.95)	x, y, z
2					
N5–H5···O666 (1)	0.880(0.004)	1.957(0.004)	2.797(0.005)	159.20(0.27)	$-x, -y+2, z-1/2$
N5–H5···O777 (1)	0.880(0.004)	2.854(0.004)	3.344(0.006)	116.81(0.27)	$-x, -y+2, z-1/2$
3					
N3–H3···O101 (0)	0.880(0.002)	2.036(0.003)	2.855(0.004)	154.24(0.16)	x, y, z
N5–H5N···O111 (0)	0.714(0.029)	2.368(0.028)	3.049(0.003)	160.11(2.81)	x, y, z
N4–H4NB···O666 (4)	0.820(0.034)	2.954(0.028)	3.134(0.003)	95.03(2.09)	$x+1/2, -y+1/2, z-1/2$
O101–H101···O777 (2)	0.620(0.045)	2.479(0.043)	2.982(0.004)	140.29(4.64)	$-x+1, -y, -z$
O101–H102···Cl2 (4)	0.849(0.032)	2.929(0.032)	3.671(0.003)	146.96(2.82)	$x+1/2, -y+1/2, z-1/2$
4					
N3–H3···O101 (1)	0.880(0.012)	2.174(0.013)	2.960(0.018)	148.42(0.99)	$-x+1, -y+1, -z+2$
N5–H5···O333 (3)	0.880(0.022)	2.413(0.013)	2.996(0.022)	124.01(1.28)	$x-1, y, z$

Table 4. EPR spectral parameters of the copper(II) complexes.

Parameter	**1**	**2**	**3**	**4**
Polycrystalline state (298 K)				
g_z	2.4018	2.3324	2.214	2.1842
g_y	2.076	2.0862	2.0663	2.0663
DMSO (77 K)				
$g_\parallel$	2.297	2.280	2.179	2.245
$g_\perp$	2.066	2.0631	2.056	2.060
$A_\parallel(G)$	149	160	193	137
G	4.5	4.4	3.2	4.0
α^2	0.686	0.757	0.735	0.612
β^2	1.035	0.902	0.892	0.843
γ^2	0.686	0.934	0.983	1.173
$K_\perp$	0.741	0.734	0.732	0.718
$K_\parallel$	0.797	0.785	0.659	0.737
f (cm^{-1})	165	149	121	175

3.5. *EPR spectra*

EPR spectra of **1–4** in polycrystalline powder at room temperature and in frozen DMSO solution were recorded. Some representative spectra are shown in "Supplementary material," figures S1 and S2. Derived EPR parameters are presented in table 4. EPR spectra of copper(II) complexes are sensitive to coordinating atoms and also to the net charge of the complexes [28]. In general, $g_\parallel$ decreases and $A_\parallel$ increases

with increasing negative charge of the ligand. EPR spectra of **1**–**4** in the solid state at 298 K and 77 K consist of $g_{\|}$ and $g_{\perp} \sim 2.0$ (figure S2), consistent with $d_{x^2-y^2}$ ground state in tetragonal ligand field. However, at 300 K, the spectra exhibit four fairly well-resolved components originating from −3/2, −1/2, 1/2, and 3/2 transition ($\Delta M_s = 1$). The $g_{\|}$ values for these complexes are in the range 2.179–2.2969 and $g_{\perp}$ values are in the range 2.056–2.066. These g values are comparable to the reported g-values [29] for similar spectra of copper(II) complexes. The value $g_{\|} < 2.3$ indicates considerable covalent character of the M–L bond [30]. In **1**–**4**, all EPR signals are shifted slightly toward higher magnetic field, leading to smaller $g_{\|}$ and $g_{\perp}$ values. This finding is in line with increased ligand field operating through $g = 2.0023 + n\xi[E_0 - E_n]$ [31]. The geometric parameter G, a measure of the exchange of interaction between the copper centers in a polycrystalline solid, has been calculated. According to Hathaway and Billing [32] if $G > 4$ the exchange interaction is negligible and $G < 4$ indicates exchange interaction. The values of G for present complexes are 4.5, 4.4, 3.2, and 4.0, respectively, for **1**, **2**, **3**, and **4**, indicating exchange interaction in solid state. From the low temperature EPR spectra, various bonding parameters such as in-plane σ-bonding, in-plane π-bonding as well as out-of-plane π-bonding were evaluated [33] by using the following expression [34].

$$\alpha^2 = \left(A_{||}/0.036\right) + (g_{||} - 2.0023) + 3/7(g_{\perp} - 2.0023) + 0.04.$$

By these values the nature of the metal–ligand bonding in these complexes can be understood. The orbital reduction factors $K_{\|}$ and $K_{\perp}$ were estimated from the expression [35]:

$$K_{\|}^2 = \left(g_{\|} - 2.0023\right)E_{\mathrm{d-d}}/8\lambda_0,$$

$$K_{\perp}^2 = (g_{\perp} - 2.0023)E_{\mathrm{d-d}}/2\lambda_0,$$

where $K_{\|} = \alpha^2\beta^2$, $K_{\perp} = \alpha^2\gamma^2$, and λ_0 represents the one electron spin–orbit coupling constant for the free ion, equal to $-828\,\mathrm{cm}^{-1}$. Significant information about the nature of bonding in the copper(II) complexes can be derived from the magnitude of $K_{\|}$ and $K_{\perp}$. In the case of pure σ bonding $K_{\|} \approx K_{\perp} \approx 0.77$ whereas $K_{\|} < K_{\perp}$ implies considerable in-plane bonding, while for out-of-plane bonding, $K_{\|} > K_{\perp}$. In the present copper(II) complexes, $K_{\|} < K_{\perp}$ indicates the presence of significant in-plane bonding. The evaluated values of α^2, β^2, and γ^2 of the complexes are consistent with both strong in-plane σ and in-plane π bonding. The computed values of α^2 and β^2 (table 4) are compared with ionic copper(II) complexes [36]. Therefore, the present complexes may be regarded as ionic. The empirical factor $f = g_{\|}/A_{\|}\,\mathrm{cm}^{-1}$ is an index of tetragonal distortions and may vary from 105 to 135 for small to extreme distortions in square-planar complexes and depends on the nature of the coordinated atoms [37]. The f values of these complexes are 165 for **1**, 150 for **2**, 121 for **3**, and 175 for **4**, indicating significant distortion from planarity. It has been observed [38] that the contribution of the 4s orbital to σ-bonding between metal and ligand donor atoms orbital is predominant in complexes having α values greater than 0.70. For these complexes, the values are near this value, which supports a ground term with purely 3d character.

3.6. *IR spectra*

IR spectral analysis shows that the (C=N) of the Schiff base shifts to lower energies in spectra of the complexes, indicating coordination *via* the azomethine nitrogen. This is confirmed by bands at 440–464 cm^{-1}, assigned to Cu–N [39]. The increase in frequency of this band in spectra of the complexes is due to increased band strength, again confirming coordination *via* the azomethine nitrogen. In all the complexes a strong band at 266–280 cm^{-1} is consistent with the Cu–N of pyridine [40]. The strong, sharp band at ~1650 cm^{-1} can be attributed to a (C=O) vibration [41]. New bands with medium to weak intensities appear at 395–405 cm^{-1} in **1**–**4**, which are tentatively assigned to (M–O)/(M–N) modes [42].

Based on the above spectral evidence, the ligand is coordinated tridentate to the metal, coordinating *via* the azomethine nitrogen, pyridyl nitrogen, and carbonyl oxygen. In **1** and **2,** these bands are sensitive to coordination and shifted to higher frequencies in the complexes with respect to the free ligands [43]. The presence of coordinated water in **1**, **2**, and **4** is indicated by a broad band at 3500–3200 cm^{-1} [44] and two weaker bands at 300–750 cm^{-1} and 720 cm^{-1} due to (OH) rocking and wagging vibrations, respectively [45]. The absence of spectral bands in this region in spectra of **3** indicates that the water in this complex is not coordinated but present as lattice water [46].

In **2**, **3**, and **4**, the bands ~1100 cm^{-1} and ~625 cm^{-1} indicate that the T_d symmetry of ClO_4^- is maintained, suggesting ClO_4^- outside the coordination sphere [47]. The IR spectra of **3** are dominated by bands due to dien [48].

3.7. *Cyclic voltammetry*

Cyclic voltammograms of $\mathbf{L^1}$ and its metal complexes are carried out in DMSO containing 0.1 mol L^{-1} $NaClO_4$ as the supporting electrolyte; the data are summarized in table 5. The cyclic voltammograms for copper(II) complexes exhibit metal-centered electrochemical process (Supplementary material, figure S3). The reduction waves

Table 5. Cyclic voltammetry data for 1 mmol L^{-1} solution of the Cu(II) complexes in DMSO containing 0.1 mol L^{-1} $NaClO_4$ as supporting electrolyte.

Complex	Scan rate	E_{pc} (mV)	I_{pc} (μA)	E_{pa} (mV)	I_{pa} (μA)	ΔE_p (mV)	$E^{0\prime}$ (mV)	I_{pa}/I_{pc} (μA)
1	100	27	3.043	270	2.053	243	148	0.67
	200	19	3.442	282	2.231	263	150	0.65
	300	11	3.469	292	2.258	281	151	0.65
2	100	−6	2.384	228	1.564	234	111	0.65
	200	−19	2.521	242	1.666	261	111	0.66
	300	−23	2.572	257	1.714	280	117	0.66
3	100	−302	1.180	29	0.779	−331	136	0.65
	200	−304	1.562	32	1.031	−336	136	0.65
	300	−306	3.431	34	2.301	−340	136	0.67
4	100	−301	1.392	30	0.891	−331	136	0.64
	200	−303	1.587	32	1.032	−335	135	0.65
	300	−305	1.988	36	1.253	−341	134	0.63

$\Delta E_p = E_{pa} - E_{pc}$; $E^{0\prime} = (E_{pa} + E_{pc})/2$.

(peak A and its oxidation counterpart peak C) are related to the Cu(II)/Cu(I) reduction in the range 0–1.4 V while on the anodic side in the range 0–1.0 V, there exists an oxidation curve (peak D) with its cathodic peak E. Peak B is related to either ligand redox or coupled chemical reactions. In all cases, peak potential difference increases as the scan rate is increased.

Analysis of the cyclic voltammetric response of peak A/C indicates that this process originates from quasireversible Cu(II)/Cu(I) redox couple with a peak-to-peak separation (ΔE_p) = 234–341 mV at 300 mVS^{-1} [49]. The separation between potential peaks may vary from 100 to 350 mV, characteristic of quasireversible process. The ratio of I_{pa}/I_{pc} is less than unity, indicative of electron transfer followed by a chemical reaction (EC mechanism) [50]. In the absence of either uncompensated solution resistance or anomalous electrode surface effects, the marked departure of ΔE from 59 mV can be reorganization accompanying the redox changes [51]. The redox potentials observed imply that rearrangement of **1**–**4** is probably due to deformation in the chelate rings of the coordinated Schiff-base hydrazone. The cyclic voltammetric behavior of **4** between 1.0 and 0 V exhibits cathodic response (peak E) from 100 to 200 mV with its counterpart (peak D) at 300–400 mV, corresponding to a quasireversible Cu(III)/Cu(II) redox process [52] as shown by ΔE values as well as the non-equivalent intensities of the cathodic and anodic peaks (I_{pa}/I_{pc}). The redox process associated with oxidation of Cu(II) to Cu(III) may originate due to the presence of pyridine and the redox active hydrazone moiety. Cu(II)/Cu(I) redox potential for effective catalysis for superoxide radical must be between $E^0 = 0.16$ V *versus* NHE (−0.405 V *vs.* SCE) for O_2/O_2^- and $E^0 = 0.89$ V *versus* NHE (−0.645 mV *vs.* SCE) for O_2^-/H_2O_2. Although it is inappropriate to compare the $E_{1/2}$ values with the reduction potentials of the couples O_2/O_2^- and O_2^-/H_2O_2, the redox potentials of the four complexes in DMF should be in the allowed ranges of an SOD mimic, and results of the SOD activity assay show that all have relatively high activity. The reduction behavior of **1**–**4** implies that $\mathbf{L^1}$ is able to accommodate the geometrical change from Cu(II) to Cu(I). This process is presumed to involve either four-coordinate or five-coordinate Cu(I).

3.8. *SOD activity*

The SOD catalytic activities toward the dismutation of superoxide anions (O_2^-) of **1**–**4** were investigated by NBT assay [52]. The chromophore concentration needed to yield 50% inhibition of the reduction of NBT is called IC_{50}. The IC_{50} values are listed in table 6 along with the kinetic constant [53]. A representative inhibition curve is shown in figure 5. Complex **3** shows highest SOD activity ($IC_{50} = 32$ μmol dm^{-3}). The difference in IC_{50} values for the four complexes should be ascribed to the different structures, especially in the conformation of the ligand. A greater interaction between superoxide and Cu(II) in mixed ligand complex is due to the stronger axial bond [54], which results in increased catalytic activity. These complexes may be considered as analogs of SOD but are somewhat less active than the native enzyme ($IC_{50} = 0.04$ μmol L^{-1}). The higher values may be due to the strong ligand field created by the tridentate Schiff base which opposes the interaction of the complexed copper with the superoxide radical; another important factor is the ability of the ligand to accommodate the reduced copper(I) center in a tetrahedral or linear environment [55]. The weaker SOD-like activity of **1**, **2**,

Table 6. IC_{50} values and kinetic catalytic constants of **1–4**.

Complex	IC_{50} (μmol)	k_{McCF} $((mol\,L^{-1})^{-1}\,s^{-1}) \times 10^4$
1	38	2.50
2	42	2.26
3	32	2.97
4	44	2.16

k_{McCF} was calculated by $K = k_{NBT} \times [NBT]/IC_{50}$, k_{NBT} (pH 7.8) $= 5.94 \times 10^4$ $(mol\,L^{-1})^{-1}\,s^{-1}$ [52].

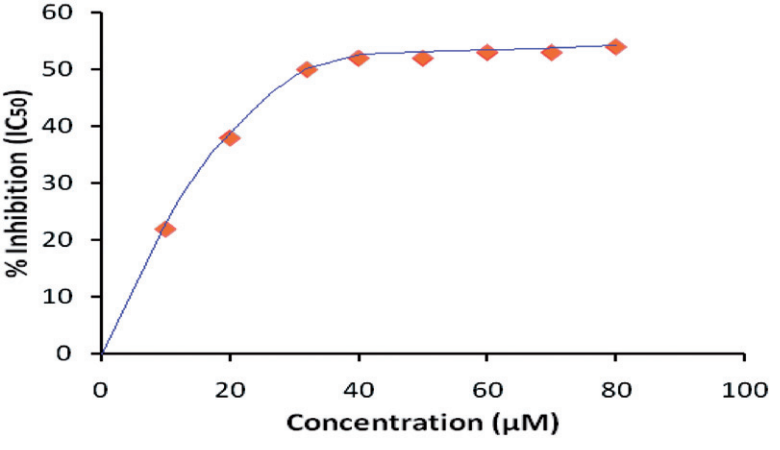

Figure 5. SOD activity of $[Cu(L^1)(Dien)](ClO_4)_2(H_2O)$ (**3**).

and **4** may be attributed to greater steric hindrance of the coordinated water [56] hindering action of O_2^-. Similar SOD activities have been reported [10, 57–59].

3.9. *Antibacterial activity*

The susceptibility of certain strains of bacteria toward $\mathbf{L^1}$ and complexes were evaluated against *Escherichia coli*, *Proteus vulgaris*, and *Staphylococcus aureus* (G+) and (G−) species of bacteria. All the copper complexes showed better antibacterial response than the respective Schiff base (table 7). The potent action of the metal complexes compared with Schiff base may be due to coordination. Complex **1** was highly active against *E. coli* (Supplementary material, figure S4). Antibacterial actions of these complexes with remaining bacteria were appreciable but lower than standard antibiotics (chloramphenicol). Complexes **2**, **3**, and **4** show moderate activity with *E. coli, P. vulgaris,* and *S. aureus* bacterial Sp. (figure 6). DMSO control has no inhibitory response. Similar antibacterial activities were reported in our previous work [10, 59]. Difference in antibacterial activity of the complexes can depend on the nature of ligands [60].

4. Conclusion

The results in this article demonstrate that careful design of a ligand can lead to an asymmetric mononuclear system, which binds copper strongly. We have synthesized

Table 7. Antibacterial activity of L^1 and **1–4**.

Complex	Concentration ($\mu g\,mL^{-1}$)	Diameter of inhibition zone (in mm)		
		E. coli	*P. vulgaris*	*S. aureus*
L^1	20	7	6	6
1	10	8	6	7
	15	10	8	9
	20	13	9	10
2	10	7	6	6
	15	9	7	8
	20	10	9	9
3	10	8	6	7
	15	9	8	9
	20	11	9	10
4	10	7	7	6
	15	8	9	7
	20	10	10	9
Chloramphenicol	10	25	23	23
DMSO (control)		Nil	Nil	Nil

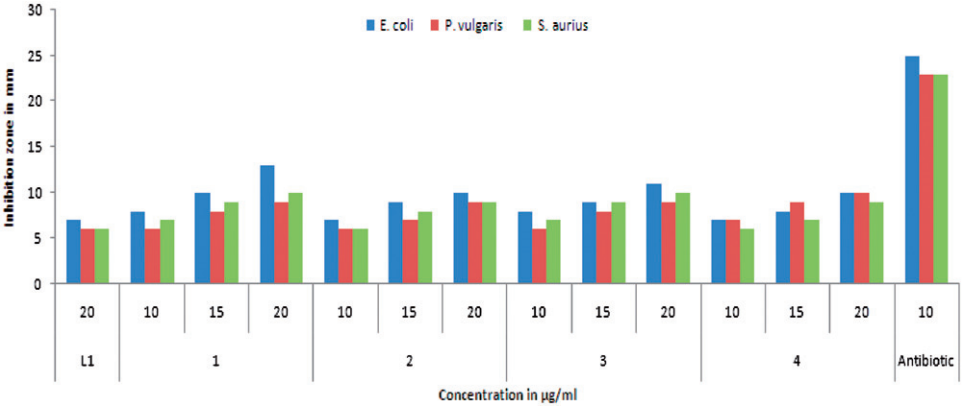

Figure 6. Graphical representation of antibacterial activities of **1–4**.

and characterized $[Cu(L^1)(Phen)(H_2O)](NO_3)_2$ (**1**), $[Cu(L^1)(bipy)(H_2O)](ClO_4)(H_2O)(NO_3)$ (**2**), $[Cu(L^1)(Dien)](ClO_4)_2(H_2O)$ (**3**), and $[Cu(L^1)(ImH)(H_2O)](ClO_4)$ (**4**). The distorted octahedral geometry of **1–3** and distorted square-pyramidal geometry in **4** are proven by single-crystal analysis. The complexes show SOD activity even though they do not have structural similarity with the native enzyme. These complexes exhibit antibacterial activity against the tested bacterial Sp.

Supplementary material

CCDC 770447, 770448, 770446, and 770445 contain the supplementary crystallographic data for $[Cu(L^1)(Phen)(H_2O)](NO_3)_2$ (**1**), $[Cu(L^1)(bipy)(H_2O)](ClO_4)(H_2O)(NO_3)$ (**2**),

$[Cu(L^1)(Dien)](ClO_4)_2(H_2O)$ (**3**), and $[Cu(L^1)(ImH)(H_2O)](ClO_4)$ (**4**) and have been synthesized with newly synthesized Schiff base derived from 2-pyridinecarboxaldehyde and benzoylhydrazine, where L = N-[(1)-pyridin-2-ylmethylidene]benzohydrazide. These data can be obtained free of charge *via* http://www.ccdc.cam.ac.uk/conts/retrieving.html, or from the Cambridge Crystallographic Data Centre, 12 Union Road, Cambridge CB2 1EZ, UK; Fax (+44) 1223-336-033; or E-mail: deposit@ccdc.cam.ac.uk

Acknowledgments

Our sincere thanks to the National Single Crystal X-ray Diffraction Facility X-ray Division and RSIC (SAIF), IIT Mumbai for single-crystal data collection and EPR measurements, respectively. The Head RSIC (SAIF), Central Drug Research Institute, Lucknow is also gratefully acknowledged for providing analytical and spectral facilities. Financial assistance from UGC [Scheme No. 36-28/2008 (SR)] and CSIR [Scheme No. 01(2451)/11/EMR-II] New Delhi are also gratefully acknowledged.

References

[1] J.A. McCleverty, T.J. Meyer. In *Comprehensive Coordination Chemistry II, From Biology to Nanotechnology*, J.A. McCleverty, T.J. Meyer (Eds), Vol. 9 (Volume editor M.D. Ward), pp. 719–758, Elsevier, Oxford, UK (2004).
[2] D.M. Beghaei, S. Mohebi. *Tetrahedron*, **58**, 5357 (2002).
[3] J.R.J. Sorrenson. *Prog. Med. Chem.*, **26**, 437 (1989).
[4] K.D. Karlin, Z. Tyekar. *Bioinorganic Chemistry of Copper*, Chapman and Hall, New York (1993).
[5] K. Drabent, A. Bioloska, Z. Ciunik. *Inorg. Chem. Commun.*, **7**, 224 (2004).
[6] A.S. Kabeer, M.A. Baseer, N.A. Mole. *Asian J. Chem.*, **13**, 496 (2001).
[7] W.M. Singh, B.C. Das. *Pesticides*, **22**, 11 (1988).
[8] S.B. Desai, P.B. Desai, K.R. Desai. *Heterocycl. Commun.*, **7**, 83 (2001).
[9] S. Samadhiya, A. Halve. *Orient. J. Chem.*, **17**, 119 (2001).
[10] R.N. Patel, A. Singh, K.K. Shukla, D.K. Patel, V.P. Sondhiya. *J. Coord. Chem.*, **64**, 902 (2011).
[11] R.N. Patel, A. Singh, K.K. Shukla, D.K. Patel, V.P. Sondhiya, S. Dwivedi. *J. Sulfur Chem.*, **31**, 299 (2010).
[12] R.N. Patel, V.L.N. Gundla, D.K. Patel. *Polyhedron*, **27**, 1054 (2008).
[13] H.B. Gray, J. Ballhausen. *J. Am. Chem. Soc.*, **85**, 260 (1963).
[14] T.E. Khalil, L. Labib, M.F. Iskander. *Polyhedron*, **13**, 2569 (1994).
[15] G.M. Sheldrick. *Acta Crystallogr. A*, **46**, 467 (1990).
[16] G.M. Sheldrick. *SHELXL-97. Program for the Refinement of Crystal Structures*, University of Göttingen, Germany (1997).
[17] I. Garcia, E. Bermejo, A.K. EI-Sawaf, A. Castineiras, W.X. West. *Polyhedron*, **21**, 729 (2002).
[18] K.D. Karlin, J.C. Hayes, S. Juen, J.P. Hutchinson, J.P. Zubieta. *J. Inorg. Chem.*, **21**, 4106 (1982).
[19] C.K. Johnson. *ORTEP, III Report ORNL-5138,* Oak Ridge National Laboratory, Oak Ridge, TN (1976).
[20] A.W. Addision, T.N. Rao, J. Reedijk, G.C. Vershoor. *J. Chem. Soc., Dalton Trans.*, 1349 (1984).
[21] P.K. Dhara, S. Pramanik, T.-H. Lu, M.G.B. Drew, P. Chattopadhyay. *Polyhedron*, **23**, 2457 (2004).
[22] K.D. Karlin, J.C. Hayes, S. Juen, J.P. Hutchinson, J. Zubieta. *Inorg. Chem.*, **21**, 4106 (1982).
[23] A.G. Bingham, H. Bagge, E.W. Ainslough, A.M. Brodie. *J. Chem. Soc., Dalton Trans.*, 493 (1987).
[24] A.B.P. Lever. *Inorganic Electronic Spectroscopy*, 2nd Edn, Elsevier, Amsterdam (1984).
[25] Y. Nakao. *Inorg. Chim. Acta*, **55**, 103 (1981).
[26] M. Nonoyamo, K. Yamasaki. *Inorg. Chim. Acta*, **5**, 124 (1971).
[27] J. Peisach, W.E. Blumberg. *Arch. Biochem. Biophys.*, **165**, 691 (1974).
[28] R.C. Chikate, S.B. Padhye. *Polyhedron*, **24**, 1689 (2005).

[29] J.P. Kilmman. *Chem. Rev*., **96**, 2541 (1996).
[30] D. Kivelson, R. Nieman. *J. Chem. Phys*., **35**, 149 (1961).
[31] R.N. Patel, N. Singh, K.K. Shukla, V.L.N. Gundla, U.K. Chauhan. *J. Inorg. Biochem*., **99**, 651 (2005).
[32] B.J. Hathaway, D.E. Billing. *Coord. Chem. Rev*., **5**, 143 (1970).
[33] R.C. Chikate, A.R. Belapure, S.B. Padhye, D.X. West. *Polyhedron*, **358**, 2023 (2005).
[34] G.F. Bryce. *J. Phys. Chem*., **70**, 3549 (1966).
[35] D.X. West. *Inorg. Nucl. Chem*., **43**, 3169 (1984).
[36] B.G. Malmstrom, T. Vanngard. *J. Mol. Biol*., **2**, 118 (1960).
[37] R.J. Rudley, B.J. Hathaway. *J. Chem. Soc*., 1725 (1970).
[38] B. Hathaway. *Struct. Bond*., **14**, 60 (1973).
[39] M.B. Ferrari, G.G. Fava, M. Lafranchi, C. Pelizzi, P. Tarasconi. *Inorg. Chim. Acta*, **181**, 253 (1991).
[40] R.J. Clark, C.S. Williams. *Inorg. Chem*., **4**, 350 (1965).
[41] J. Borras, G. Alznet, M. Gonzatez-Alvarez, F. Estevan, B. Macias, M. Liu-Gonzatez, A. Cast. *Polyhedron*, **26**, 5009 (2007).
[42] K. Nakamoto. *Infrared and Raman Spectra of Inorganic and Co-ordination Compounds*, 2nd Edn, Wiley-Interscience, New York, NY (1970).
[43] K.N. Lazarou, I. Chadjlstamaths, A. Terzis, S.P. Perlepes, C.P. Raptopoulou. *Inorg. Chim. Acta*, **363**, 107 (2010).
[44] G. Singh, P.A. Singh, H. Singh, D.P. Singh, R.N. Hand, S.N. Dubey. *Proc. Natl. Acad. Sci. Ind*., **72A**, 87 (2002).
[45] P.R. Shukla, V.K. Singh, A.M. Jaiswal, J. Narain. *J. Ind. Chem. Soc*., **60**, 321 (1983).
[46] K. Nakamoto. *Infrared and Raman Spectra of Inorganic and Co-ordination Compounds*, 5th Edn, Wiley, New York (1997).
[47] B.J. Hathaway, A.E. Underhill. *J. Chem. Soc*., 3091 (1961).
[48] C.A. Bolos, P.V. Fanourgakis, P.C. Chrisdis, G.S. Nikolov. *Polyhedron*, **18**, 1661 (1999).
[49] G. Tabbi, W.L. Driessen, J. Reedijk, R.P. Bonomo, N. Veldman, A.L. Spek. *Inorg. Chem*., **36**, 1168 (1997).
[50] D.H. Evans. *Chem. Rev*., **90**, 739 (1990).
[51] A.R. Handrickson, R.L. Martin, N.M. Rhode. *Inorg. Chem*., **15**, 2115 (1976).
[52] N. Raman, S. Ravichandran, C. Thangaraja. *J. Chem. Sci*., **116**, 215 (2004).
[53] R.P. Pasternnack, B. Helliwell. *J. Am. Chem. Soc*., **101**, 1026 (1979).
[54] J.P. Collman, T.R. Halbert, K.S. Suslickin, T.G. Spiro. *Metal Ion Activation of Dioxygen*, p. 1, Wiley, New York (1980).
[55] S. Praveen, F. Arjmand. *Indian J. Chem*., **44A**, 1151 (2005).
[56] J. Han, Y. Xing, C. Wang, P. Hon, F. Bai, X. Zeng, X. Zhang, M. Ge. *J. Coord. Chem*., **62**, 745 (2009).
[57] M. Patel, D. Gandhi, P. Parmar. *J. Coord. Chem*., **64**, 1276 (2011).
[58] R.N. Patel, A. Singh, K.K. Shukla, D.K. Patel, V.P. Sondhiya, S. Dwivedi. *J. Coord. Chem*., **63**, 3483 (2010).
[59] R.N. Patel, K.K. Shukla, A. Singh, M. Choudhary, D.K. Patel. *J. Coord. Chem*., **63**, 586 (2010).
[60] B.G. Tweedy. *Phytopathology*, **55**, 910 (1964).